

Gravitational Lensing Limits on the Average Redshift of Gamma-Ray Bursts

Daniel E. Holz

Department of Physics, University of Chicago
5640 South Ellis Avenue, Chicago, IL 60637-1433
deholz@rainbow.uchicago.edu

M. Coleman Miller

Department of Astronomy and Astrophysics, University of Chicago
5640 South Ellis Avenue, Chicago, IL 60637-1433
miller@bayes.uchicago.edu

Jean M. Quashnock

Department of Astronomy and Astrophysics, University of Chicago
5640 South Ellis Avenue, Chicago, IL 60637-1433
jmq@oddjjob.uchicago.edu

ABSTRACT

The lack of bright host galaxies in several recently examined gamma-ray burst (GRB) error boxes suggests that the redshifts of cosmological GRBs may be significantly higher than previously hypothesized. On the other hand, the non-detection of multiple images in the BATSE 4B catalog implies an upper limit to the average redshift $\langle z \rangle$ of GRBs. Here, we calculate an upper limit to $\langle z \rangle$, independent of the physical model for GRBs, using a new statistical lensing method that removes distance ambiguities, and thus permits accurate computation of the lensing rate at high z . The upper limit on $\langle z \rangle$ depends directly on the cosmological parameters Ω and Λ . If there are no multiple images among the brightest 80% of the first 1802 bursts in the BATSE 4B catalog, then, at the 95% confidence level, $\langle z \rangle < 2.2, 2.8, 4.3, \text{ or } 5.3$ for (Ω, Λ) values of $(0.3, 0.7)$, $(0.5, 0.5)$, $(0.5, 0.0)$, or $(1.0, 0.0)$, respectively. The 68% upper limit to the average redshift is comparable to or less than the median redshift of GRBs in scenarios in which the GRB rate is proportional to the rate of star formation, for any cosmology. The uncertainty in the lensing rate—arising from uncertainties in the cosmological parameters and in the number density and average velocity dispersion of galaxies—will be reduced significantly in the next few years by a new generation of experiments and surveys. Moreover, the continued increase in the number of GRBs observed by BATSE will greatly constrain their redshift distribution.

Subject headings: cosmology: observations — gamma rays: bursts — gravitational lensing — methods: numerical

1. INTRODUCTION

Three decades after their discovery (Klebesadel, Strong, & Olson 1973), the physical origin of gamma-ray bursts (GRBs) remains unresolved. Recent developments, however—including the isotropy of GRBs seen by BATSE (Briggs et al. 1996; Tegmark et al. 1996) and the detection of redshift $z=0.835$ absorption and emission lines from a possible optical counterpart to GRB 970508 (Metzger et al. 1997; Reichart 1998)—strongly suggest a cosmological origin for GRBs.

Initially, no-evolution fits to the $\log N - \log P$ (peak flux) distribution of BATSE GRBs suggested a typical redshift of $z \sim 1$ for dim bursts (Fenimore et al. 1993; Wickramasinghe et al. 1993), with the break in the $-3/2$ slope of the flux distribution at $P \sim 10 \text{ ph cm}^{-2} \text{ s}^{-1}$ being interpreted as a cosmological deviation from Euclidean space at $z \sim 1$. In addition, a number of researchers reported a factor of ~ 2 “time-stretching” of dim bursts relative to bright ones (e.g., Norris et al. 1994, 1995), which was thought to imply a redshift of order unity for the dim bursts. Such a redshift would imply an extremely low rate of gravitational lensing and multiple imaging of sources detected with BATSE, perhaps as low as one multiple imaging event per 200 years (Grossman & Nowak 1994).

New lines of evidence now indicate that the typical redshift of cosmological GRBs may substantially exceed unity. Particularly suggestive evidence for high GRB redshifts comes from deep HST searches of the error boxes of several of the brightest GRBs detected by BATSE and the Interplanetary network (IPN): In five cases, no obvious host galaxies for the bursts were found, down to a limiting magnitude between 3.5 and 5.5 mag fainter than what would be expected if GRBs reside in L_* galaxies and dim bursts are at $z \sim 1$ (Schaefer et al. 1997). This “no-host problem” has been analyzed further by Band & Hartmann (1998), and implies that if GRBs reside in normal galaxies, even the *brightest* of them are at redshifts close to unity, with the faintest being at much higher redshift still. In addition, Fenimore & Bloom (1995) showed that the intrinsic anticorrelation between photon energy and burst duration implies that if the observed time-stretching is caused by time dilation, then the redshift of the dimmest bursts may be as large as $z \sim 6$ (note, however, that some or all of the time-stretching may be intrinsic to the bursts; cf. Stern, Poutanen, & Svensson 1997).

These new lines of evidence have led researchers to explore scenarios in which the bursts are at much higher redshifts. One currently popular scenario, motivated in part by the assumption that cosmological GRBs involve remnants of massive stars, is that the GRB rate is proportional to the rate of (massive) star formation (Totani 1997; Wijers et al. 1998). The star formation rate is thought to vary strongly with redshift (Madau et al. 1996), peaking at $z \sim 2$. If this is the case, the dimmest bursts may be at redshift $z \sim 6$, making them the most distant objects ever detected (Wijers et al. 1998). Other authors have noted that, if the comoving number density of GRB sources is allowed to vary with redshift, then even if the peak luminosity is fixed, the $\log N - \log P$ distribution and other properties of the BATSE bursts can be fit by models with a maximum redshift up to $z \sim 10\text{--}200$ (Rutledge, Hui, & Lewin 1995).

In these high- z scenarios, the expected incidence of gravitational lensing and multiple imaging of GRB sources is much higher than it is in lower- z scenarios, since in general the lensing rate increases markedly with the source redshift. The short duration of GRBs (typically tens of seconds) compared to the difference in light travel time between different ray paths (typically months, if the lens is of galactic mass; cf. Mao 1992) means that a multiply-imaged GRB appears as two or more separate events with identical time histories and intensities that differ only by a scale factor. The image separations, of order arcseconds, are tiny compared to BATSE location errors; thus, these GRBs would appear to come from the same location.

Two or more such events must be detected in order to identify a lensed GRB source; thus, the overall BATSE burst detection efficiency, ϵ , is of prime importance in determining the observed incidence of lensing. The average efficiency for the 4B catalog is $\epsilon = 0.48$ (Meegan et al. 1998), which is 40% larger than the previously estimated value (Fishman et al. 1994). This increase implies that the expected incidence of lensing is significantly higher than was previously believed.

Lensing of GRBs was first suggested by Paczynski (1986) as a way to establish their cosmological origin. Subsequently, many authors have calculated the lensing rate of GRBs (Mao 1992; Blaes & Webster 1992; Nemiroff et al. 1993; Grossman & Nowak 1994), assuming GRB redshifts estimated from no-evolution fits to the $\log N - \log P$ distribution, viz., $z \lesssim 1$. For redshifts $z \lesssim 1$, the gravitational lensing rate is reasonably well known for a given cosmology (e.g., Turner, Ostriker, & Gott 1984; Fukugita & Turner 1991; Fukugita et al. 1992). At redshifts $z \gtrsim 1$, however, the lensing rate has been uncertain, mainly because of ambiguity in the angular diameter distance at high redshift (Fukugita et al. 1992). As a result, even when the cosmology and the number density and properties of lenses are fixed, the estimated lensing rate can vary by factors of several between the different prescriptions.

Motivated in part by this ambiguity, Holz & Wald (1998) have developed a numerical method to calculate lensing rates for a given cosmology, combining techniques from both “ray-shooting” and “Swiss-cheese” models. The approach resolves the angular-diameter distance uncertainties, and also correctly accounts for multiple lens encounters along the line of sight, allowing for an unambiguous calculation of lensing rates.

If there are no multiple images among the bursts detected with BATSE, then an upper limit to the average redshift $\langle z \rangle$ of GRBs can be inferred, one which depends directly on the cosmological parameters (see also Nemiroff et al. 1994; Marani et al. 1998; Marani 1998). Here, we set an upper limit to $\langle z \rangle$, independent of the physical model for GRBs, using the Holz & Wald (1998) method to compute the lensing rate for a variety of cosmologies.

The plan of this paper is as follows. In § 2 we describe and develop the statistical lensing method, and compare its results with analytical estimates. We show that analytical estimates using the “filled-beam” approach are reasonably accurate for source redshifts less than $\sim 2-3$, but underestimate the true rate of lensing by tens of percent at higher redshifts. In § 3 we use the numerical method to compute the lensing rate as a function of redshift for several cosmologies,

and compare these results with previous estimates. We also determine upper limits on the rate of lensing and on the average redshift $\langle z \rangle$ of GRBs, assuming that no lensing events are present in the BATSE 4B catalog (Meegan et al. 1998). We discuss the implications of these results and give our conclusions in § 4. We follow the conventions that the Hubble constant is $100 h \text{ km s}^{-1} \text{ Mpc}^{-1}$, Ω is the present mean density in the universe in units of the closure density, and Λ is the present normalized cosmological constant. In a flat universe, $\Omega + \Lambda = 1$.

2. GRAVITATIONAL LENSING RATE CALCULATIONS

We utilize a recently developed numerical model (Holz & Wald 1998) to calculate the lensing rate. This method offers a number of distinct advantages over previous lensing treatments. The model is fully described and discussed in Holz & Wald (1998), and we refer the reader to that paper for details. In § 2.1 we give an overview of the features of this method relevant to the calculations reported here, and in § 2.2 we compare the numerical results to analytic lensing rates and lens redshift distributions.

2.1. Overview of Statistical Lensing Method

In current analytic methods (see, e.g., Turner et al. 1984; Fukugita et al. 1992), every lensing event is treated as a photon beam traveling through a universe described by a given angular diameter distance expression, and encountering a single lens at some point along its path. These methods require distance measures to calculate lensing probabilities. Common angular diameter distance measures include the Dyer-Roeder empty- and filled-beam expressions (Dyer & Roeder 1972, 1973), and the Ehlers & Schneider (1986) variant of these expressions. The empty-beam distance assumes that the photon beams encounter no mass aside from that of the lenses, and otherwise travel through vacuum. The filled-beam distance presupposes that, aside from the lenses, the beams encounter exactly the Robertson-Walker mass density at every point along their trajectories. These Dyer-Roeder expressions assume that the rays travel far from all clumps of matter. The Ehlers-Schneider expression attempts to take into account the statistical effects of a clumpy universe. At higher redshifts ($z > 1$), the differences in lensing rates inferred from the different distance measures can be large, and there is no natural way to select between the differing results. A further assumption in most analytic treatments is that the lensing is dominated by a single encounter (Turner et al. 1984). It has been unclear to what extent this is a reasonable assumption, especially at higher redshifts where the probability of multiple close encounters becomes large.

For these reasons it is necessary to look at numerically determined lensing rates, which in general include multiple lens encounters, and, by integrating along ray-paths in model universes, are able to eliminate the need for averaged distance expressions. In particular, the method we use

resolves ambiguities by calculating the distances of a given photon beam directly, bypassing the need for an averaging expression. In addition, our method considers every encounter along the line of sight, with contributions from thousands of possible lenses for a given source.

The model we utilize can be thought of as a combination of Swiss-cheese models (Kantowski 1968) and ray shooting models (Premadi, Martel, & Matzner 1998; Wambsganss, Cen, & Ostriker 1998). As in the Swiss-cheese approach, we decompose the universe into comoving spherical regions, and allow for mass inhomogeneities within each region. Unlike most Swiss-cheese treatments, however, we do not require an opaque core radius, and we permit arbitrary mass distributions within the comoving spheres. As is done in ray-shooting approaches, we develop statistics by considering many random rays. However, by appropriately treating every individual region along the line of sight, we avoid the need to collapse the matter near the beam into lensing planes, as is commonly done in current ray-shooting approaches.

Rather than constructing an image out of many different photons, we calculate the effects for an infinitesimal bundle of photons (commonly called a *beam*). Instead of using the geodesic equation for each individual photon component of an image, we use the geodesic deviation equation for the beam as a whole, and track the lensing parameters for a given image along a single null geodesic. We compute the area, shear, and rotation of each beam as a function of redshift. Because these beams represent random directions on the sky, a large number of such beams constitutes a sample of the past light cone of an observer.

For our purposes, the *area* of the beam is the quantity of greatest interest, as it is inversely proportional to the magnification of the corresponding image. On occasion the area goes to zero at some point along a beam’s path (and then becomes negative, representing an inversion of the image). This is a *caustic*, and once this has happened the photon beam represents a secondary image. For every secondary image, there exists another beam that connects the source and observer without a caustic. This latter image is the primary image, and one of these exists for *every* source. The probability that a randomly selected source is multiply imaged is thus related to the probability that a randomly selected photon beam has a caustic. Most lensing events are dominated by a single encounter with a lens, and in these cases pairs of images are produced. If one assumes that all multiple images are pairs (see §§ 3 and 4 below), then, by determining the fraction of beams which have a caustic, it is possible to compute the probability for multiple imaging, and hence the lensing rate.

The model describes the universe, on *all* scales, by a Robertson-Walker metric that is perturbed by a weak Newtonian potential ϕ :

$$ds^2 = -(1 + 2\phi)d\tau^2 + (1 - 2\phi)a^2 \left[\frac{dr^2}{1 - kr^2} + r^2(d\theta^2 + \sin^2\theta d\varphi^2) \right], \quad (1)$$

where τ , r , θ , and φ are the usual Robertson-Walker coordinates, $a(\tau)$ is the cosmological expansion factor, and the curvature of the spatial part of the metric is either open ($k = -1$), flat

($k = 0$), or closed ($k = 1$). We assume that the Newtonian potential ϕ is small (weak-field), that accelerations are non-relativistic, and that linear curvature terms dominate the non-linear ones:

$$\begin{aligned} |\phi| &\ll 1 \\ |\partial\phi/\partial\tau|^2 &\ll D^a\phi D_a\phi \\ (D^a\phi D_a\phi)^2 &\ll D^b D^c\phi D_b D_c\phi, \end{aligned}$$

where D_a is the spatial derivative operator of the metric of equation (1), and where the summation is over all spacetime indices.

As shown in Holz & Wald (1998), the Einstein equations for this metric are globally described by the standard evolution equations for Robertson-Walker cosmologies. Locally, however, this metric is equivalent to a Minkowski spacetime that is weakly perturbed by a Newtonian potential. As we are solely interested in the statistical distributions of photon beams (and, in particular, in scenarios where strong lensing is rare), we do not need to consider correlations between photon beams. The matter distribution in the universe far from a photon’s trajectory is not relevant to the lensing, and need not even be known (Holz & Wald 1998). We therefore restrict our consideration to matter in the immediate vicinity of the beam. With this in mind, we choose a maximum clustering scale, \mathcal{R} , for the cosmological matter. For the purposes of this paper we have chosen $\mathcal{R} = 2$ Mpc, to correspond to typical galaxy separations. We divide the mass of the universe into spheres of comoving radius \mathcal{R} , each representing an individual galaxy. These spheres contain a certain amount of Robertson-Walker matter, with a given distribution for the matter within each sphere. As discussed in Holz & Wald (1998), clustering on larger scales does not significantly affect the rate of lensing by galaxies¹ (clustering does produce lensing by larger masses, typically 10^{14} – $10^{15} M_\odot$, but the time delay between images for such lensing is longer than the few year baseline of BATSE observations, and hence we neglect it in our analysis). We have restricted ourselves to distributions in the form of truncated singular isothermal spheres. Although we could allow these to evolve in time, in what follows we have taken the mass distributions to be static; we do not consider evolution of the lenses (see § 4).

The path of a photon beam in this model universe can be broken into many steps, with lensing effects due solely to the nearest galaxy calculated at each step. The distance a photon traverses at any particular step is determined by the impact parameter with which the photon enters the appropriate sphere (representing the local galaxy neighborhood). At no point do we need to arbitrarily specify an average distance measure, as the distance for each photon beam is

¹Press & Gunn (1973) showed that the lensing rate from point masses (and, in general, from objects with mass entirely within their Einstein radii) is a function solely of the total mass in the point masses, and is independent of their mass distribution. On the other hand, if the matter is not confined to within its Einstein radius, then only the Ricci contribution to lensing matters. This contribution is completely local and is thus independent of clustering on scales much less than the observer-source distance. We thus expect our results to be independent of the value of \mathcal{R} , and to depend only on the total amount of mass in lenses. Indeed, we find that our results with $\mathcal{R} = 4$ Mpc are the same as those with $\mathcal{R} = 2$ Mpc.

calculated individually. We consider a photon beam that starts at the observer ($z = 0$), and trace its path backwards in time. It enters the first sphere (representing the first galaxy encountered) of radius \mathcal{R} , with a random impact parameter. We calculate the lensing of the beam due to the mass distribution within the sphere. After traversing the sphere, the photon proceeds to the next galaxy along its path, again with a random impact parameter. As it traverses the boundaries between spheres, the effects of the cosmological contraction and blueshift (we are heading backwards in time) are taken into account. This process is continued from one galaxy to the next, yielding the lensing parameters of the photon beam as a function of redshift. We repeat this process for many different photons, in each case generating random impact parameters for every galaxy encounter. Each photon beam is thus completely uncorrelated with all others, and can be thought to randomly sample a distinct direction on the sky. By this Monte-Carlo tracing of photon beams, lensing rates can be calculated for a given cosmology. In this paper a typical simulation will involve tracing the paths of $\sim 10^4$ independent photon beams.

A detailed discussion of the lensing rate results from the above method, including a comparison with results commonly found in the literature, will be reported elsewhere. In the following subsection we present results for a number of cosmologies of interest, and discuss their main features.

2.2. Comparison of Numerical Results with Analytical Forms

We compare the lensing probability and distribution of lens redshifts given by the numerical method described above with the filled-beam values, for several different cosmologies. Figure 1 shows the lensing rates for $\Omega=0.3, \Lambda=0.7$; $\Omega=0.5, \Lambda=0.5$; $\Omega=0.5, \Lambda=0$; and $\Omega=1, \Lambda=0$. These curves are constructed assuming that the dimensionless parameter $F \equiv 16\pi^3 n_0 R_0^3 (\sigma_{\parallel}/c)^4$ is equal to 0.1, where n_0 is the comoving number density of galaxies, $R_0 = c/H_0$, and σ_{\parallel} is the velocity dispersion inside the galaxies.

A striking feature of the data displayed in Figure 1 is the good agreement, for redshifts $z \lesssim 3$, between the numerical results and the results obtained from the analytic filled-beam expressions. At redshifts much less than unity, the difference between filled- and empty-beam results are slight; all distance measures yield similar lensing rates. Hence, agreement in this regime is expected. But at higher redshifts, such a close agreement is not expected *a priori*. Why is it obtained?

We note that a small F parameter corresponds to galaxies extending well outside their Einstein radii. Matter outside the Einstein radius contributes to lensing solely through its Ricci contribution to the convergence of a beam. This is a local effect, and thus in this case the lensing of a beam depends upon the amount of matter that the beam traverses (see, e.g., Holz & Wald 1998). For $F = 0.1$, $\Omega = 0.5$, and $\Lambda = 0$, for example, isothermal galaxies have halo radii of ≈ 200 kpc. The Einstein radii of these objects is $\approx 2-5$ kpc, depending on the redshifts of the source and lens, so roughly 98% of the matter contributes to lensing solely through Ricci effects;

hence the concordance between our numerical results and the analytic filled-beam expressions.

At much higher redshifts ($z \gtrsim 3$), the numerical results begin to deviate from the filled-beam expressions, yielding larger lensing rates. At these high redshifts the incidence of multiple lens encounters becomes significant (Press & Gunn 1973; Pei 1993). For lower redshifts, lensing encounters are invariably dominated by a single lens, because the probability of multiple close lens encounters is negligible. However, at higher redshifts multiple close passes become more common, and these are expected to *increase* the overall lensing rate. Consider, for example, an encounter in which a beam skims just outside the Einstein radius of a lens, picking up a significant amount of convergence, but not quite enough to generate a caustic. If this beam then comes close to another lens, it is possible for the additional convergence from this second lens to cause the beam to caustic. Although neither of the lens encounters would have yielded multiple imaging by themselves, their combined contribution can cause a secondary image to appear. Thus, the presence of multiple lenses is expected to increase the lensing rate. A thorough analysis of the contribution of multiple lenses to lensing will be reported elsewhere.

Figure 2 shows the distribution of lens redshifts in a universe with $\Omega=0.3$ and $\Lambda=0.7$, for a source at $z=3$ (panel a) and for a source at $z=5$ (panel b), as well as for $\Omega=1$ and $\Lambda=0$ (panels c and d). The histograms give the numerically determined distribution, and the solid lines give the analytical form in the filled-beam approximation. Again the numerical answers agree reasonably well with the analytical estimates. We note that in all cases the bulk of the lenses are at $z \sim 1$.

3. UPPER LIMITS ON GRB REDSHIFTS FROM LACK OF LENSING

3.1. Calculation of the expected number of lensed events

In § 2 we used the statistical lensing method (Holz & Wald 1998) to compute the probability $\tau(z)$ that a point source at redshift z is multiply imaged. This quantity is dependent on the cosmological parameters, Ω and Λ , as well as parameters describing the model for the lenses. We have taken for such a model the *singular isothermal sphere* (SIS) model (see, e.g., Turner et al. 1984; Fukugita & Turner 1991; Kochanek 1993a), wherein the lens is the spherically symmetric gravitational potential of a massive dark matter halo of constant temperature. The lensing probability $\tau(z)$ then depends directly on the parameter F , defined in § 2. For realistic models, $0.05 < F < 0.15$; for definiteness, we take $F = 0.1$ (§4, see below).

In the SIS model, the lensing event always consists of two images—the third central image is far too faint to be observed—with a time delay Δt between the two images of order months for lenses of galactic mass (Mao 1992; Grossman & Nowak 1994). Thus (§4) we take a constant BATSE efficiency $\epsilon = 0.48$ (Meegan et al. 1998) to see either image, and ϵ^2 to see *both*.

Let N_{tot} be the total number of *observed* bursts: For the 5.5 yr observing period of the BATSE 4B catalog (Meegan et al. 1998), $N_{\text{tot}} = 1802$. There are then approximately N_{tot}/ϵ *actual* burst

sources above the BATSE threshold during this time. If these sources are all at a given redshift z , the expected number N of image pairs is:

$$N = (N_{\text{tot}}/\epsilon) \cdot \epsilon^2 \cdot \tau(z) = \epsilon N_{\text{tot}} \tau(z) . \quad (2)$$

Of course, not all the burst sources are at the same redshift. If instead the burst sources distribution in redshift is given by $C(z)$, where $C(z)$ is the fraction of burst sources with redshift less than z , we then have:

$$N = \epsilon N_{\text{tot}} \int_0^\infty dC(z) \tau(z) . \quad (3)$$

Furthermore, not all lensed images are actually observable: In some cases the images will be too faint to be detected by BATSE (Grossman & Nowak 1994). We must include the effect of image magnification (or de-magnification) on the expected number of lenses in equation (3).

We define b_{min} as the brightness threshold below which identification of burst lenses from lightcurve comparison is impossible. (Throughout this paper, we measure brightness in units of peak flux [ph cm⁻² s⁻¹] averaged over 1024 ms and for energies between 50 and 300 keV.) Consider a lensed burst from a source at redshift z , with apparent *unlensed* brightness b . What is the conditional probability that both images are then brighter than the threshold b_{min} ?

The magnification μ_- of the fainter of the two images is $\mu_- = (r_{\text{E}}/r_s) - 1$, where r_{E} is the Einstein radius and r_s the impact parameter (see, e.g., Grossman & Nowak 1994). Thus the fainter image will be brighter than b_{min} only if $r_s/r_{\text{E}} < (1 + b_{\text{min}}/b)^{-1}$, so that the conditional probability we seek is $(1 + b_{\text{min}}/b)^{-2}$. With $F_z(b)$ the fraction of bursts at redshift z with apparent unlensed brightness brighter than b , the expected number N of *observable* image pairs is now:

$$N = \epsilon N_{\text{tot}} \int_0^\infty dC(z) \tau(z) \int_0^\infty dF_z(b) \frac{1}{[1 + b_{\text{min}}/b(z)]^2} . \quad (4)$$

Since the distribution of burst source redshifts, $C(z)$, is unknown, we compute the expected number $N_{\langle z \rangle}$ of observable image pairs as a function of $\langle z \rangle$, the *effective* average redshift, imagining that all sources are at this redshift:

$$N_{\langle z \rangle} = \epsilon N_{\text{tot}} \tau(\langle z \rangle) \int_0^\infty dF(b) \frac{1}{(1 + b_{\text{min}}/b)^2} . \quad (5)$$

Equating the two previous equations serves as a definition for the effective redshift $\langle z \rangle$ of the burst distribution, and parametrizes our ignorance of the burst source distribution $C(z)$. We take the unlensed brightness distribution, $F(b)$, to be the observed BATSE brightness distribution, since *de facto* no burst lensing has been found.

We define the integral in equation (5) to be $f(b_{\min})$, the fraction of image pairs having both images above the lightcurve–comparison brightness threshold, b_{\min} . This fraction is the conditional probability $(1 + b_{\min}/b)^{-2}$ that both images are brighter than the threshold, weighted over the actual brightness distribution, $F(b)$, for the entire BATSE sample. Figure 3 shows $f(b_{\min})$ as a function of b_{\min} (in units of peak flux), computed using the peak flux distribution $F(b)$ from the BATSE 4B catalog (Meegan et al. 1998).

In estimating the effective feasibility of lightcurve comparison of image pair candidates, previous investigators have found that as many as 90% of GRBs are bright enough for such a task (Nowak & Grossman 1994). This would imply that $b_{\min} = 0.27 \text{ ph cm}^{-2} \text{ s}^{-1}$ (Meegan et al. 1998), and that $f(b_{\min}) = 0.57$. In this work, we take a more conservative (and round) value of $f(b_{\min}) = 0.5$. This requires only that the brightest 80% of GRBs have lightcurves that can effectively be compared for lens candidate identification, a condition that is likely to be satisfied (see below).

3.2. Results and upper limits

Figure 4 shows the expected number, $N_{\langle z \rangle}$, of observable image pairs in the BATSE 4B catalog, as a function of the effective average redshift, $\langle z \rangle$, of GRB sources in the catalog. We have used equation (5) and $\tau(z)$ from § 2, and have taken $F=0.1$ and $f(b_{\min})=0.5$. We show our results for several different cosmologies.

Because $\tau(z)$ is a monotonically increasing function of z (see Figs. 1 and 2), $N_{\langle z \rangle}$ is also a monotonically increasing function of $\langle z \rangle$. Hence, if there are no multiply imaged GRB sources in the BATSE 4B catalog, there is a corresponding upper limit to $\langle z \rangle$.

To date, Marani et al. (1998) and Marani (1998) have compared the lightcurves of the brightest 75% of the first 1235 BATSE bursts and find no match among any of them. Thus there is no evidence of gravitational lensing in these bursts. The limits for $\langle z \rangle$ that we quote in this paper consider the 1802 bursts in the BATSE 4B catalog, assuming that 80% of them are bright enough for analysis and none of those 80% are multiply imaged. The heavy dashed horizontal lines in Figure 4 indicate the 68% (lower line) and 95% (upper line) confidence limits to the number of lensing events allowed in the BATSE 4B catalog.

The intersection points for these confidence limits are given in Table 1, giving the 68% and 95% confidence-level upper limits on the effective average redshift $\langle z \rangle$ for several different cosmologies. The strongest limits arise in cosmologies with a large cosmological constant, where the lensing rate is quite high: At the 95% confidence level, we find that $\langle z \rangle < 2.2$ if $\Lambda = 0.7$ and $\Omega = 0.3$. The weakest limit arises in an Einstein–de Sitter universe, where the lensing rate is smallest: At the 95% confidence level, we find that $\langle z \rangle < 5.3$.

In Table 1 we also give the limits that result from the current analysis of 1235 bursts (Marani

et al. 1998; Marani 1998), and those that would arise if no lensing events are seen in a sample twice the current size, namely 3600 bursts. Such a sample can be produced if BATSE continues to operate in its current fashion for another five years. Note that the resultant limits are much smaller and less dependent on the cosmological parameters, so that the continued increase in the number of GRBs observed by BATSE will greatly constrain their redshift distribution (see § 4).

Assuming no lensing in the current BATSE sample, we find that the 68% upper limit on $\langle z \rangle$, as a function of the cosmological parameters, is approximately given by:

$$\langle z \rangle < 1.5 + (\Omega - \Lambda) \pm 0.1 . \quad (6)$$

This confirms the quasi-degeneracy in the lensing rate (see, e.g., Kochanek 1993b) as a function of the cosmological parameters, so that our upper limits are dependent on the difference $\Omega - \Lambda$. Studies of high-redshift supernovae (see, e.g., Perlmutter et al. 1997, 1998; Garnavich et al. 1998) also constrain $\Omega - \Lambda$: This is not surprising, since their results are also based upon the redshift-distance relation. Riess et al. (1998) find a best-fit value for $\Omega - \Lambda$ of -0.5 , with a systematic error of approximately ± 0.3 . Systematic errors arising from reddening corrections could in principle allow the supernova data to be consistent with $\Omega - \Lambda$ as large as $+0.4$, but preliminary indications are that these corrections are small (A. Riess, private communication). Hence the 68% upper limit on $\langle z \rangle$ is less than 1.9, and is probably close to 1.0. Current star-formation models, for which $\langle z \rangle \sim 2.2$, are marginally inconsistent (1σ) with our limits, regardless of the cosmology. If $\Omega - \Lambda < -0.4$, these models are inconsistent with our limits at the 2σ level.

These upper limits to $\langle z \rangle$, combined with the median fluence of $10^{-5} \text{erg cm}^{-2}$ of the BATSE bursts (see Meegan et al. 1998) imply that, at the 68% confidence level, the upper limit to the median rest-frame energy release of the BATSE gamma-ray bursts is between $1.8 \times 10^{52} h^{-2}$ ergs (for $\Omega = 0.3$ and $\Lambda = 0.7$) and $2.9 \times 10^{52} h^{-2}$ ergs (for $\Omega = 1$ and $\Lambda = 0$) for the energy observed in the BATSE window, where the energy is assumed to be emitted into 4π steradians.

4. DISCUSSION AND SUMMARY

We have exhibited a new method for calculating gravitational lensing rates, given a cosmology and a distribution and evolution of the lenses. This method, which is described more fully in Holz & Wald (1998), is free of the angular diameter distance ambiguity that is a feature of standard analytical methods. For the cosmologies and redshift ranges we have examined, we find that the lensing rate is approximately equal to the filled-beam lensing rate for $z < 3$, but in excess of the filled-beam rate for $z > 3$. We find that the lack of detected lensing in the current BATSE catalog places an upper limit to the median redshift of bursts that, at the 68% confidence level, is comparable to or less than the median redshift in star-formation burst models.

We now discuss these results and place them in context. In § 4.1 we discuss the simplifying

assumptions that have been made in our calculation. We find that these assumptions have, if anything, caused us to *underestimate* the lensing rate. In § 4.2 we examine the uncertainties in the inputs used in our calculations, as well as the future prospects for reducing these uncertainties. In § 4.3 we discuss the implications of the current lack of lensing for cosmological models of gamma-ray bursts, when combined with existing lower bounds to the redshift of bursts in these models. Finally, in § 4.4 we provide a future outlook for the rapidly emerging importance of constraints inferred from detection or nondetection of lensing.

4.1. Effects of Simplifying Assumptions

We have assumed that the angular distribution of the sources of gamma-ray bursts is uncorrelated with the angular distribution of the lenses. This is well justified, because for sources at low redshift the lenses that contribute most to the lensing rate are at about half the redshift to the source, and for sources at high redshift the dominant lenses are at a redshift of approximately unity (see § 2; see also, e.g., Turner et al. 1984; Mao 1992). Hence, in a cosmological model the sources of gamma-ray bursts are separated from lenses by hundreds of megaparsecs to gigaparsecs, and therefore it is extremely unlikely that the sources and lenses are angularly correlated. We have also assumed that the phase of the orbit of BATSE is uncorrelated between the separate images of the burst, and hence that the joint probability of two images being observable is just the square of the BATSE efficiency, $0.48^2 \approx 0.23$. This assumption is reasonable if the time delay between images is significantly larger than the BATSE orbit time of ~ 5000 seconds. The time delay for a mass M is of order $10^{-5}(M/M_\odot)$ seconds (see, e.g., Blandford & Narayan 1992), and hence the assumption of uncorrelated phases is good for masses $M \gtrsim 10^9 M_\odot$. This includes almost all the effective lensing mass of galaxies, and thus this assumption is also unlikely to affect the calculated lensing rates significantly.

We may have underestimated the lensing rate by assuming that only galaxies—which we have modeled as singular isothermal spheres—contribute to the lensing rate. Nemiroff et al. (1993) have noted that point masses, for example supermassive black holes, could also in principle contribute. To produce gamma-ray burst lensing of the type that we consider here, in which the lensing event appears as two separate bursts, the mass of such a lensing black hole must be $M \gtrsim 10^8 M_\odot$, because smaller masses would produce time delays less than ~ 1000 seconds, so that overwriting or readout time would tend to prevent BATSE from detecting two separate bursts (the effect of lensing by lower-mass black holes may, however, be detectable using techniques such as autocorrelation analysis; see Nemiroff et al. 1994, 1998). If, however, the total lensing rate were dominated by very massive black holes, $M \gtrsim 10^{10} M_\odot$, then these objects would also produce detectable image separation of lensed quasars or galaxies (the angular separation is of order $3(M/M_\odot)^{1/2}(D/1\text{Gpc})^{-1/2} \mu\text{arcsec}$ for an Einstein ring, which is $0.3''$ for $M = 10^{10} M_\odot$ and $D=1$ Gpc). Hence, the amount by which we have underestimated the lensing rate depends on the number of point masses in the relatively narrow range 10^8 – $10^{10} M_\odot$, which is the only mass range

that could avoid detection in quasar lensing surveys and yet produce separately detected bursts.

We may also have underestimated the lensing rate by only keeping track of the total number of images, not whether there are, e.g., two or four images in a particular event. As pointed out by Grossman & Nowak (1994), this tends to underestimate the *detectable* rate of lensing because when there are several images it is more probable that at least two of them are observed by BATSE: assuming a 48% efficiency for any particular image, the probability of observing at least one pair rises from 23% when there are two images to 66% when there are four images. Grossman & Nowak (1994) estimate that, for galaxy ellipticities typical of galaxy surveys, the maximum possible enhancement of the lensing detection rate is $\sim 30\%$, but that the overall enhancement is likely to be smaller.

A third effect that may enhance the rate of lensing is magnification bias, which is an effect first discussed extensively by Fukugita & Turner (1991) in the context of quasar lensing. Magnification bias occurs because sources that would have been undetectable are made visible by lensing, and hence a magnitude-limited sample contains an enhanced incidence of lensing. This can be especially important if the number of sources at a given flux rises steeply at the faint end, as it does in quasars. To detect multiple images and thus confirm strong lensing, it is necessary to detect the fainter image as well as the stronger image. For persistent sources such as quasars, this can be done by following up broad, shallow surveys by deep pointings, so that essentially all of the secondary images are detectable (e.g., as in the Hubble Snapshot Survey [Bahcall et al. 1992; Maoz et al. 1992, 1993a,b]). For transient sources such as gamma-ray bursts, deep follow-ups are not always possible, and hence for the secondary image to be detectable it must have a brightness in excess of the threshold of the original survey (i.e., in the case of gamma-ray bursts, the BATSE sample). This effect, plus the flatness of the faint end of the gamma-ray burst $\log N - \log P$ curve, suggests that the magnification bias for gamma-ray bursts is probably less than the magnification bias for quasars (see also Grossman & Nowak 1994 for a discussion of this point). Nonetheless, magnification bias for gamma-ray bursts could in principle increase significantly the expected lensing rate, and hence decrease the upper limits on $\langle z \rangle$, compared to the conservative estimates here.

We may underestimate the lensing rate because we have neglected the clustering of galaxies, the last of our assumptions. The enhanced gravitational potential in clusters tends to increase the convergence of null geodesics and hence increase the cross section for strong lensing (see also Holz & Wald 1998). Numerical estimates suggest that the lensing rate for galaxies in a cluster will be increased by $\sim 10\text{--}20\%$ by this effect, but because only $\sim 10\%$ of galaxies are in clusters this effect is unlikely to increase the overall lensing rate significantly.

Finally, however, we may have overestimated the rate of lensing by ignoring evolution in the properties of the lensing galaxies. If the comoving density in lensing galaxies was less in the past than it is now, or if these galaxies were less massive than they are today, high-redshift lenses would contribute less to the lensing rate than we have assumed. Note, however, that the peak in the lens

redshift distribution is at about unity (Fig. 2), when galaxies had properties very similar to their current properties. Note also that observations of lensing of quasars (see below), which have a typical redshift similar to the proposed typical redshift $z \sim 2$ of GRBs, suggest that if there are evolutionary effects then these effects have not had a dominant effect on the lensing rate.

To summarize, the net effect of our simplifying assumptions is likely to be that we underestimated the lensing rate by $\lesssim 10\%$, and hence our results are conservative in that they give a slightly high upper bound to $\langle z \rangle$.

4.2. Uncertainties in Input Parameters

In addition to the simplifying assumptions discussed above, our calculations are clearly dependent on the input values we have assumed. One input is the dimensionless parameter F , which is proportional to the product of the number density of galaxies and the fourth power of their average velocity dispersion. The lensing rate scales linearly with F . We have used $F=0.1$, which is consistent with the recent estimates from the Century Survey (Geller et al. 1997). Other estimates range from $F=0.05$ to $F=0.15$, and if these other estimates are used then the range of possible maximum redshifts is increased for a given cosmology. Fundamental cosmological parameters, another input to our calculations, are also uncertain. A standard Einstein-De Sitter universe ($\Omega=1$, $\Lambda=0$) gives the lowest lensing rate, and a Λ -dominated universe gives the highest.

Current observation of quasar lensing puts constraints on the allowed combinations of F and cosmology. For example, five of the 351 quasars in the HST Snapshot Survey (Maoz et al. 1993b) were lensed. A comparison of this rate with the rate expected for models is complicated by effects such as magnification bias (see above). However, the high average redshift of the quasars ($z \sim 2$) means that many of the issues affecting lensing of gamma-ray bursts, such as evolution of clustering, also affect the lensing of quasars. Hence, quasar lensing statistics have bearing on estimated GRB lensing rates, and will become even more relevant as more extensive surveys are done.

In addition, all of these uncertainties will be diminished greatly by the data that emerge from the plethora of satellites and surveys planned for the next few years. The number density and velocity distribution of galaxies (and hence F) will be determined with unprecedented accuracy by surveys such as 2dF (Colless 1998) and the Sloan Digital Sky Survey (Margon 1998), the latter of which is expected to see first light in 1998. Data from these surveys will also provide valuable information about Ω , Λ , clustering, and the lensing rate of quasars. Complementary information about cosmological parameters will be extracted from high-redshift supernova surveys (Perlmutter et al. 1998) and from data gathered by the many upcoming microwave background experiments, such as MAP (Wang, Spergel, & Strauss 1998), TOPHAT (Martin et al. 1996), and PLANCK (see, e.g., Bond, Efstathiou, & Tegmark 1997 for a discussion of the constraints). The evolution of galaxy clustering is already being inferred from cluster surveys, and AXAF observations of X-ray

emission from clusters of galaxies is expected to greatly enhance this understanding. Hence, one side effect of the coming data-rich era in cosmology is that calculations of lensing rates will be much less uncertain, and therefore upper limits to the redshift of a population such as gamma-ray bursts will be far more secure.

4.3. Current Implications for Cosmological GRB Models

The redshift limits presented in this paper have important consequences for cosmological models of GRBs. Lower limits on the redshift of bright GRBs are becoming stronger as the number of detected bursts rises, both because of the no-host problem (Schaefer et al. 1997) and because GRBs do not show any evidence of large-scale clustering (Lamb & Quashnock 1993; Quashnock 1996). These limits suggest that if the sources of GRBs are in or near galaxies, the median redshift of the bursts detected with BATSE may be significantly greater than unity. However, the upper limits to the redshift of GRBs that follow from the lack of lensing are beginning to make such high-redshift populations less appealing. For example, the lack of lensing in the current BATSE catalog strongly rules out the $z \sim 10$ –200 models that were heretofore consistent with the properties of the BATSE bursts (Rutledge et al. 1995). Also, models in which the burst rate is proportional to the star formation rate (Totani 1997; Wijers et al. 1998), and for which $\langle z \rangle \sim 2.2$, are beginning to be constrained strongly by the lack of lensing: Our 68% upper limit on $\langle z \rangle$ (eq. [6]) is less than 1.9, and probably close to 1.0. If the redshift upper limits are reduced further, it may be necessary to postulate either a very short interval in which GRBs were produced, with an intrinsic brightness distribution that matches the observed $\log N - \log S$ distribution, or a population that is unassociated with any known population of objects, so that the lower limits to redshift do not apply.

4.4. Future Outlook and Summary

In the next few years gravitational lensing is likely to play a role of rapidly increasing importance in constraining cosmological models of gamma-ray bursts. As discussed in § 4.2, the uncertainties in the calculation of the expected lensing rate will be diminished greatly, and hence the limits will be robust. In addition, as BATSE continues to detect bursts the statistics will steadily improve, and in the current high-redshift models lensing is to be expected in the next few years. In five years, the sample will be roughly double the ~ 1800 bursts considered here, and therefore if lensing continues to be absent, upper limits on the redshift will become extremely restrictive. At the same time, the improved statistics will continue to increase the lower limits on redshift, if there is no apparent large-scale clustering (Lamb & Quashnock 1993; Quashnock 1996). Moreover, the accurate positional estimates of BeppoSAX, HETE II, and the Fourth Interplanetary Network (IPN) are likely to provide ~ 100 error boxes of area a few square arcminutes or less in the next five years.

If instead lensing *is* detected, there will be many important consequences. For one, the cosmological origin of a particular GRB will be established from gamma-ray data for the first time (as opposed to from the afterglow, as may be the case for GRB 970508 [Metzger et al. 1997]). The approximate mass of the lens, and hence its luminosity, can be estimated from the time delay between images. The sharp peak in the probable redshift of lenses (see § 2) would then give a reasonably accurate estimate of the flux of the lens. If the GRB can be reasonably well-localized (e.g., with the IPN), this will allow a search for the lens. If the lens is found, the GRB source must essentially be angularly coincident with it, because the deflection angle is only about $1''$, and thus counterpart searches will be facilitated greatly. Knowledge of the redshift of the lens, combined with H_0 and an independent estimate of the mass of the lens (e.g., from its luminosity or velocity dispersion) will allow use of the time delay to estimate the redshift of the source. The quantifiable diversity of gamma-ray burst light curves (Marani et al. 1998; Marani 1998) means that false positives are unlikely, and hence even a single lensing event will generate a wealth of data.

In conclusion, the increased estimates of the redshift of gamma-ray bursts that were forced by the no-host problem, in addition to the greatly improved statistics of bursts and the increase in the estimate of the BATSE burst detection efficiency from 34% to 48%, mean that gravitational lensing limits are now playing a prominent role in constraining gamma-ray burst models. The role of lensing will become dramatically more important and robust in the next five years.

We thank Don Lamb for a careful reading of the manuscript and for discussions of the importance of multiple encounters. We also acknowledge valuable discussions with Bob Wald and Asantha Cooray. We thank the referee, Bob Nemiroff, for a number of helpful comments. This work was supported in part by NSF grant PHY 95-14726 (DEH), by NASA grant NAG 5-2868 (MCM), and by NASA grant NAG 5-4406 and NSF grant DMS 97-09696 (JMQ).

REFERENCES

- Bahcall, J. N., Maoz, D., Doxsey, R., Schneider, D. P., Bahcall, N. A., Lahav, O., & Yanny, B. 1992, *ApJ*, 387, 56
- Band, D. L., & Hartmann, D. H. 1998, *ApJ*, 493, 555
- Blaes, O. M., & Webster, R. L. 1992, *ApJ*, 391, L63
- Blandford, R. D., & Narayan, R. 1992, *ARA&A*, 30, 311
- Bond, J. R., Efstathiou, G., & Tegmark, M. 1997, *MNRAS*, 291, L33
- Briggs, M. S., et al. 1996, *ApJ*, 459, 40
- Colless, M. 1998, *Phil. Trans. Roy. Soc. Lon. A*, in press (astro-ph/9804079)
- Dyer, C.C. & Roeder, R.C. 1972, *ApJ*, 174, L115
- . 1973, *ApJ*, 180, L31
- Ehlers, J., & Schneider, P. 1986, *A&A*, 168, 57
- Fenimore, E. E., et al. 1993, *Nature*, 366, 40
- Fenimore, E. E., & Bloom, J. S. 1995, *ApJ*, 453, 25
- Fishman, G. J. 1994, *ApJS*, 92, 229
- Fukugita, M., & Turner, E. L. 1991, *MNRAS*, 253, 99
- Fukugita, M., Futamase, T., Kasai, M., & Turner, E. L. 1992, *ApJ*, 393, 3
- Garnavich, P. M., et al. 1998, *ApJ*, 493, L53
- Geller, M. J., Kurtz, M. J., Wegner, G., Thorstensen, J. R., Fabricant, D. G., Marzke, R. O., Huchra, J. P., Schild, R. E., & Falco, E. E. 1997, *AJ*, 114, 2205
- Grossman, S. A., & Nowak, M. A. 1994, *ApJ*, 435, 548
- Holz, D. E., & Wald, R. 1998, *Phys. Rev. D*, 58, 063501
- Kantowski, R. 1968, *ApJ*, 155, 89
- Kantowski, R., Vaughan, T., & Branch, D. 1995, *ApJ*, 447, 35
- Klebesadel, R. W., Strong, I. B., & Olson, R. A. 1973, *ApJ*, 182, L85
- Kochanek, C. S. 1993a, *ApJ*, 419, 12

- Kochanek, C. S. 1993b, MNRAS, 261, 453
- Lamb, D. Q., & Quashnock, J. M. 1993, ApJ, 415, L1
- Madau, P., Ferguson, H. C., Dickinson, M. E., Giavalisco, M., Steidel, C. C., & Fruchter, A. 1996, MNRAS, 283, 1388
- Mao, S. 1992, ApJ, 389, L41
- Maoz, D., Bahcall, J. N., Schneider, D. P., Doxsey, R., Bahcall, N. A., Lahav, O., & Yanny, B. 1992, ApJ, 394, 51
- Maoz, D., Bahcall, J. N., Doxsey, R., Schneider, D. P., Bahcall, N. A., Lahav, O., & Yanny, B. 1993a, ApJ, 402, 69
- Maoz, D., et al. 1993b, ApJ, 409, 28
- Marani, G. F. 1998, Ph.D. thesis (George Mason University)
- Marani, G. F., Nemiroff, R. J., Norris, J. P., Hurley, K., & Bonnell, J. T. 1998, in Proc. of the 4th Huntsville Gamma-Ray Burst Symposium: AIP Proceedings # 428, ed. C. A. Meegan, R. D. Preece, & T. M. Koshut, (AIP Press, New York), p. 166
- Margon, B. 1998, Phil. Trans. Roy. Soc. Lon. A, in press (astro-ph/9805314)
- Martin, N. et al. 1996, Proc. SPIE Vol 2807, Space Telescopes and Instruments IV, ed. P. Y. Bely and J. B. Breckinridge, p. 86
- Meegan, C. A. et al. 1998, <http://www.batse.msfc.nasa.gov/data/grb/4bcatalog>
- Metzger, M. R., Djorgovski, S. G., Steidel, C. C., Kulkarni, S. R., Adelberger, K. L., & Frail, D. A. 1997, IAUC 6655
- Nemiroff, R. J., et al. 1993, ApJ, 414, 36
- Nemiroff, R. J., Wickramasinghe, W. A. D. T., Norris, J. P., Kouveliotou, C. Fishman, G. J., Meegan, C. A., Paciesas, W. S., & Horack, J. 1994, ApJ, 432, 478
- Nemiroff, R. J., Norris, J. P., Bonnell, J. T., & Marani, G. F. 1998, ApJ, 494, L173
- Norris, J. P., et al. 1994, ApJ, 424, 540
- Norris, J. P., et al. 1995, ApJ, 439, 532
- Nowak, M. A., & Grossman, S. A. 1994, ApJ, 435, 548
- Paczyński, B. 1986, ApJ, 308, L43
- Pei, Y. C. 1993, ApJ, 403, 7

- Perlmutter, S., et al. 1997, *ApJ*, 483, 565
- Perlmutter, S., et al. 1998, *Nature*, 391, 51
- Premadi, P., Martel, H., & Matzner, R., *ApJ* 493, 10
- Press, W.H., & Gunn, J.E. 1973, *ApJ*, 185, 397
- Quashnock, J. M. 1996, *ApJ*, 461, L69
- Reichart, D. E. 1998, *ApJ*, 495, L99
- Riess, A. G., et al. 1998, *AJ*, in press (astro-ph/9805201)
- Rutledge, R. E., Hui, L., & Lewin, W. H. G. 1995, *MNRAS*, 276, 753
- Schaefer, B. E., Cline, T. L., Hurley, K. C., & Laros, J. G. 1997, *ApJ*, 489, 693
- Stern, B., Poutanen, J., & Svensson, R. 1997, *ApJ*, 489, L41
- Tegmark, M., Hartmann, D. H., Briggs, M. S., & Meegan, C. A. 1996, *ApJ*, 468, 214
- Totani, T. 1997, *ApJ*, 486, L71
- Turner, E. L., Ostriker, J. P., & Gott, J. R. 1984, *ApJ*, 284, 1
- Wambsganss, J., Cen, R., & Ostriker, J. P. 1998, *ApJ*, 494, 29
- Wang, Y., Spergel, D. N., & Strauss, M. A. 1998, *ApJ*, 510, in press (astro-ph/9802231)
- Wickramasinghe, W. A. D. T., Nemiroff, R. J., Norris, J. P., Kouveliotou, C., Fishman, G. J., Meegan, C. A., Wilson, R. B., & Paciesas, W. S. 1993, *ApJ*, 411, L55
- Wijers, R. A. M. J., Bloom, J. S., Bagla, J. S., & Natarajan, P. 1998, *MNRAS*, 294, L13

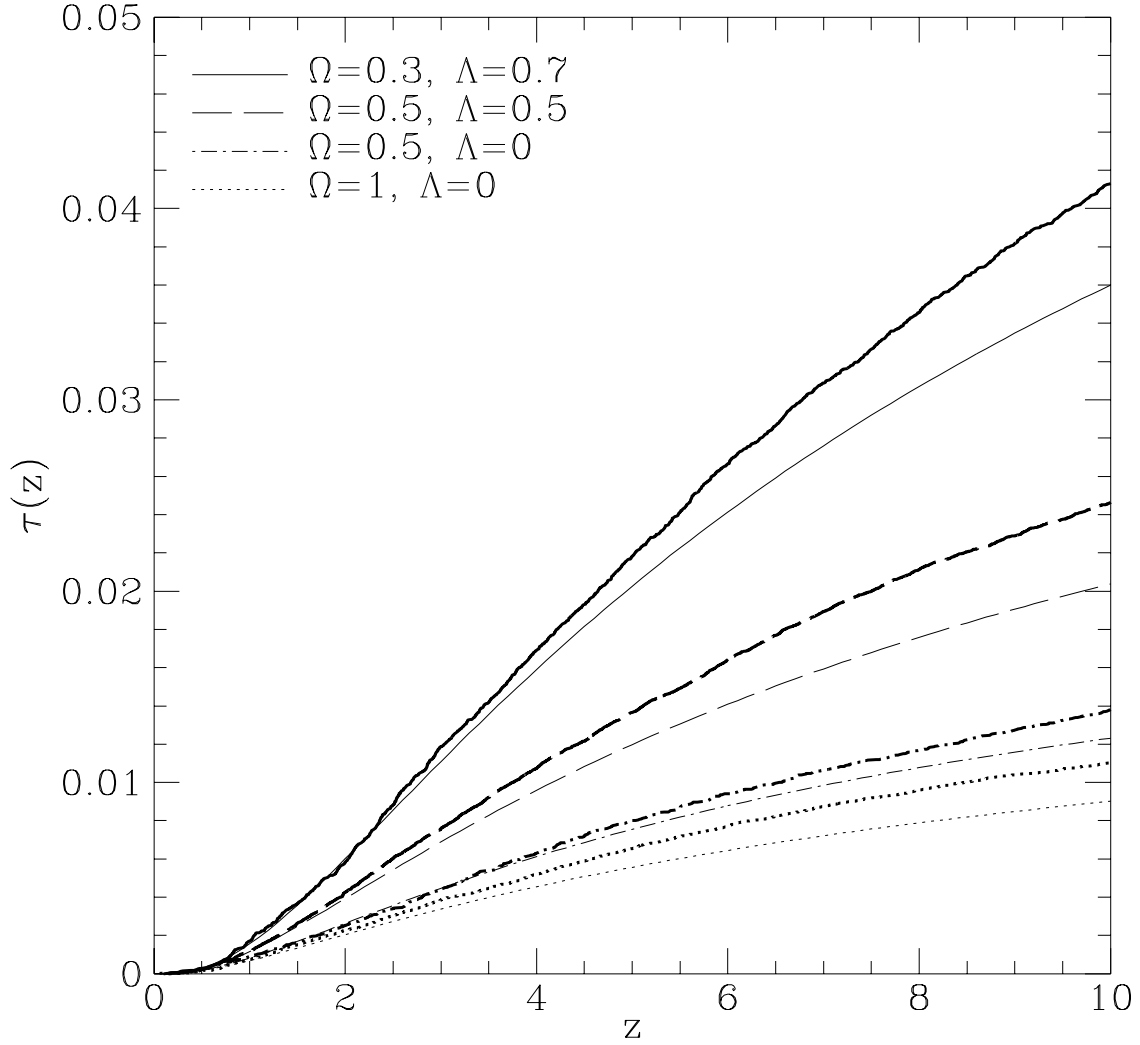


Fig. 1.— Lensing probability, $\tau(z)$, as a function of redshift, z , for a range of different cosmologies. The lenses are singular isothermal spheres, and the dimensionless parameter $F = 0.1$ (see text). The values of Ω and Λ for each curve are indicated by the legend. The boldface curves are the numerical lensing rates calculated using the procedure described in § 2. The light curves are the analytic rates calculated using the filled-beam approximation, which yields curves much closer to the numerical rates than the empty-beam (Dyer & Roeder 1973) or Ehlers-Schneider (Ehlers & Schneider 1986) prescriptions.

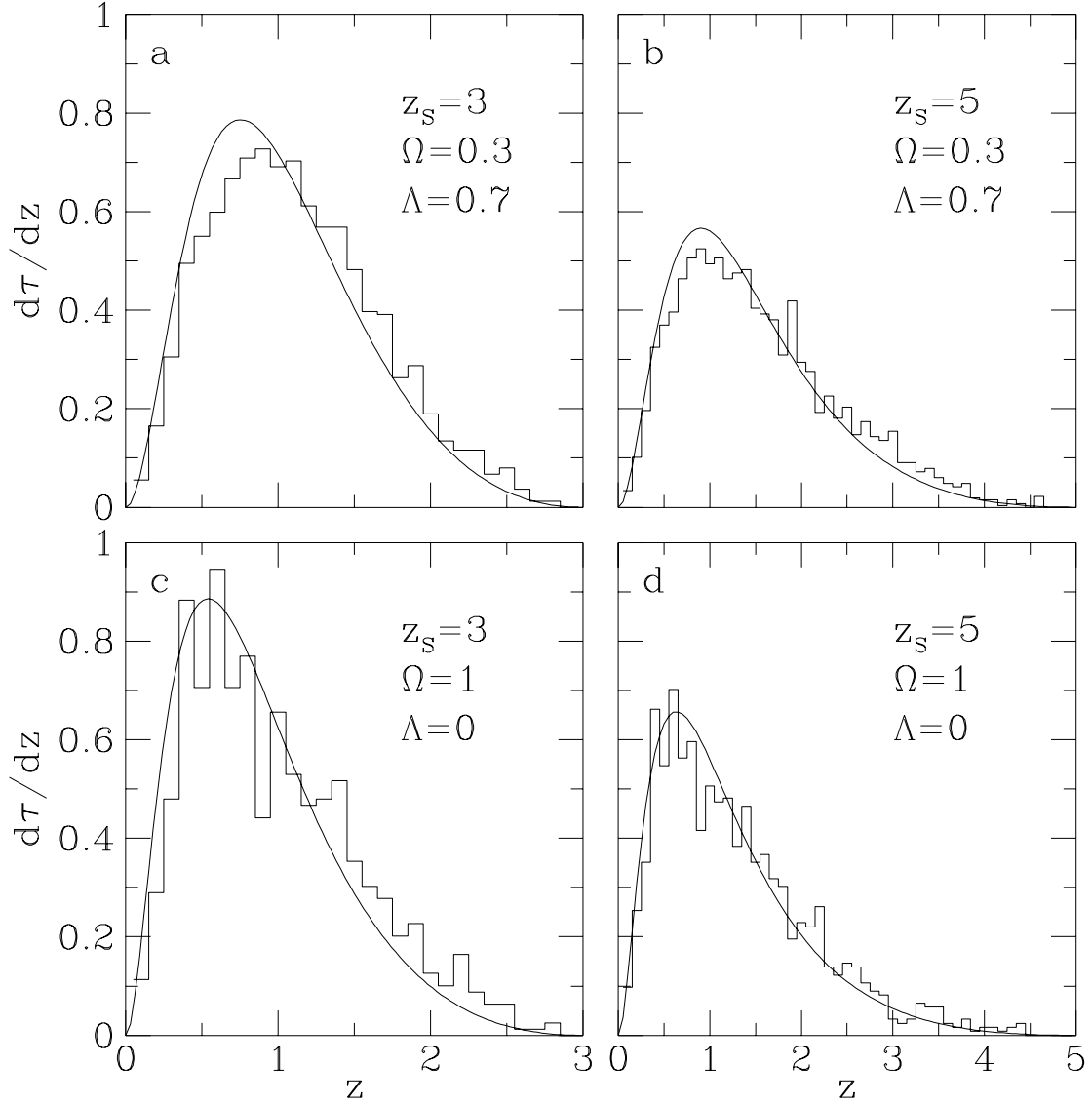


Fig. 2.— Differential redshift distribution of lenses, $d\tau/dz$, for $\Omega=0.3$ and $\Lambda=0.7$ and a source redshift of $z_s=3$ (panel a) or $z_s=5$ (panel b), and for $\Omega=1$ and $\Lambda=0$ with $z_s=3$ (panel c) or $z_s=5$ (panel d). The histograms give the numerical distribution, and the solid curves give the analytic distribution in the filled-beam approximation (Turner et al. 1984). The lenses are singular isothermal spheres.

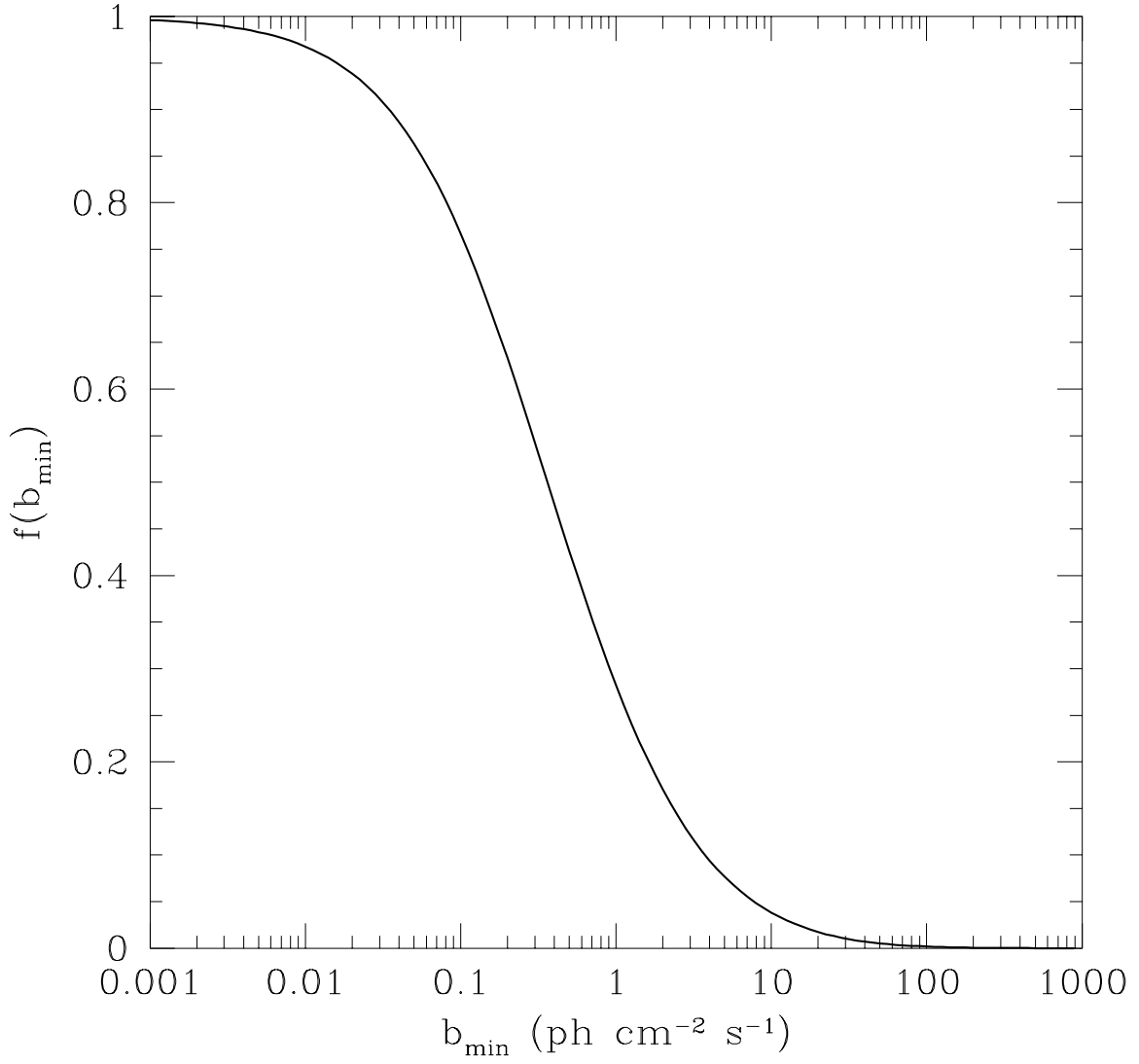


Fig. 3.— The fraction of image pairs, $f(b_{\min})$, having both images above the lightcurve-comparison brightness threshold, b_{\min} (in units of peak flux averaged over 1024 ms).

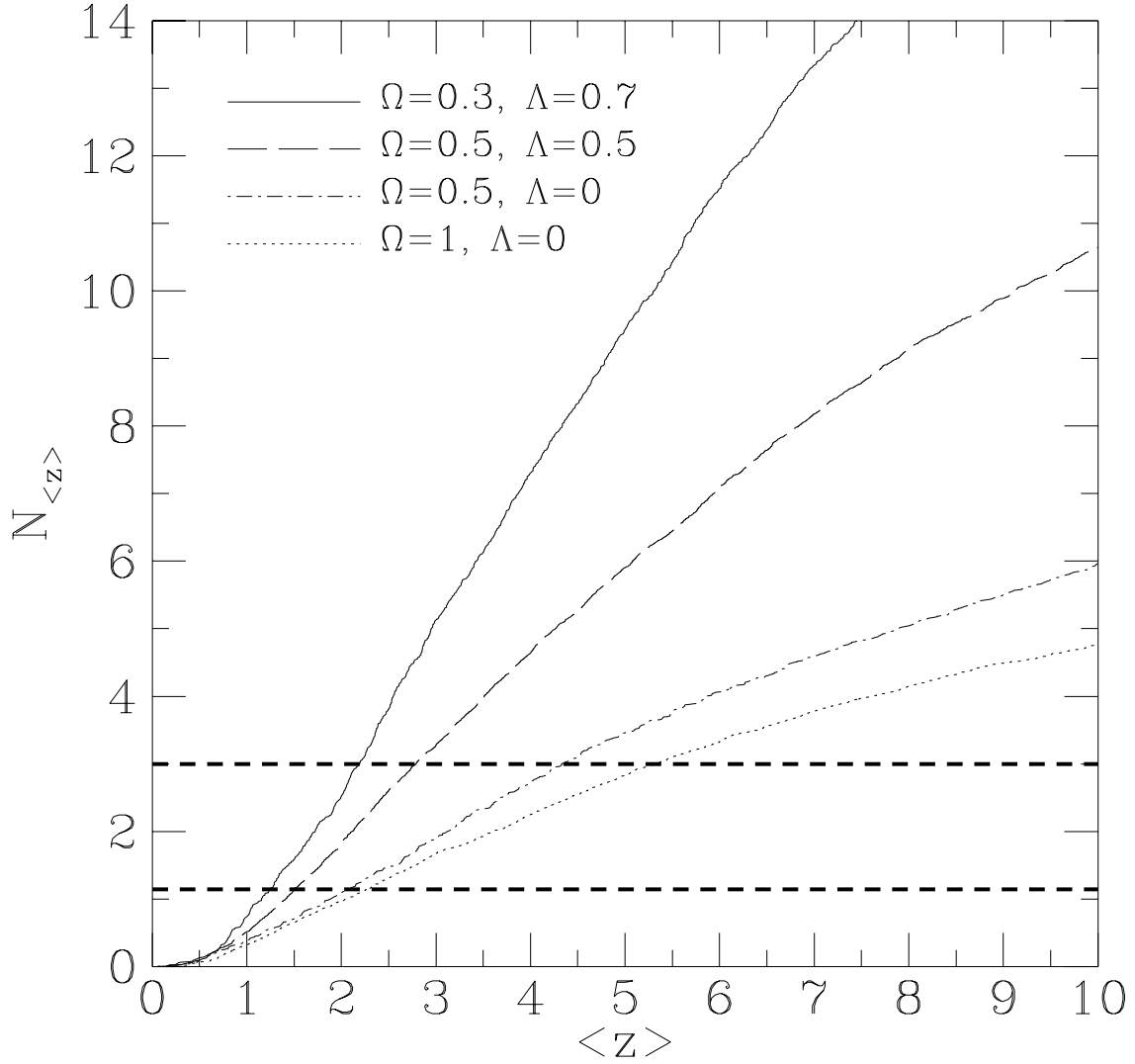


Fig. 4.— Expected number, $N_{\langle z \rangle}$, of observable image pairs in the BATSE 4B catalog, as a function of $\langle z \rangle$, the *effective* average redshift of GRB sources in the catalog, assuming that $F=0.1$ and $f(b_{\min})=0.5$. The values of Ω and Λ for each cosmology are indicated by the legend. The heavy dashed horizontal lines indicate the lensing rates that are discrepant with the lack of detected lensing at the 68% (lower line) and 95% (upper line) level.

Table 1. Limits on the average redshift $\langle z \rangle$ for different cosmologies

Confidence Level	$\Omega=0.3, \Lambda=0.7$	$\Omega=0.5, \Lambda=0.5$	$\Omega=0.5, \Lambda=0.0$	$\Omega=1, \Lambda=0$
Current analysis (1235 bursts)				
95%	2.7	3.8	6.6	8.6
68%	1.5	1.9	2.7	3.0
Current data (1802 bursts)				
95%	2.2	2.8	4.3	5.3
68%	1.2	1.5	2.1	2.3
3600 bursts with no lensing				
95%	1.4	1.8	2.6	2.8
68%	0.9	1.1	1.3	1.4